

X-Ray Spectroscopy of Young Supernovae

Vikram Dwarkadas (University of Chicago)

J. Quirola-Vasquez (MAS, PUC Chile)

F. E. Bauer (MAS, PUC Chile)

C. Badenes (U Pittsburgh)

W.N. Brandt (PSU)

T. Nymark (Stockholm)

D. Walton (Cambridge)

We gratefully acknowledge:

NASA ADAP Grant NNX14AR63

Chandra Grants GO1-12095A, GO2-13092B, GO4-15075X and GO7-18066X

X-Ray Supernovae (1995)

Table 3. Supernovae detected in the X-ray band.

SN name	Galaxy	Date of optical max	B magnitude at max	SN type	Galaxy distance ^a	X-rays first observed	Satellite used
SN 1978K	NGC 1313	~1978 June 10 ^b ~1978 May 25 ^b	~13 ~14.5	IIL IIP	4.5 Mpc	+~12.1 y	ROSAT, Asuka
SN 1980K	NGC 6946	1980 Nov 5	11.5	IIL	5.1 Mpc	+35 d	Einstein
SN 1986J	NGC 891	1983 Jan? ^c	?	Ipec	9.6 Mpc	?	ROSAT
SN 1987A	LMC	1987 May 9	3.5	IIP	50 ± 3 kpc	+154 d	Ginga
SN 1993J	NGC 3031	1993 Apr 18	11.4 ^d	Ipec	3.63 ± 0.34 Mpc	+5 d	ROSAT, Asuka, GRO

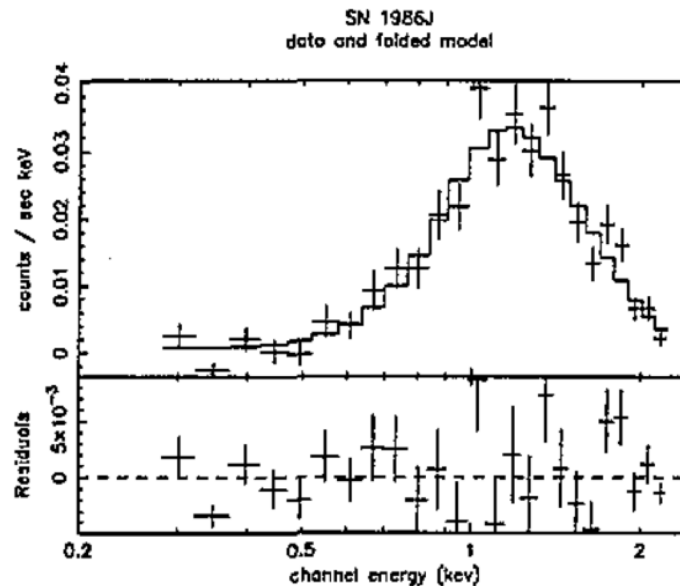
^a Distances from: SN1978K, deVaucouleurs 1963; SN1980K, deVaucouleurs 1979; SN1986J, Tully 1988; SN1987A, numerous; SN1993J, Freedman *et al* (1993).

^b Assume each type II subtype, matching optical light curve to average SN II optical behaviour to derive date of maximum (Ryder *et al* 1993a).

^c Chevalier (1987).

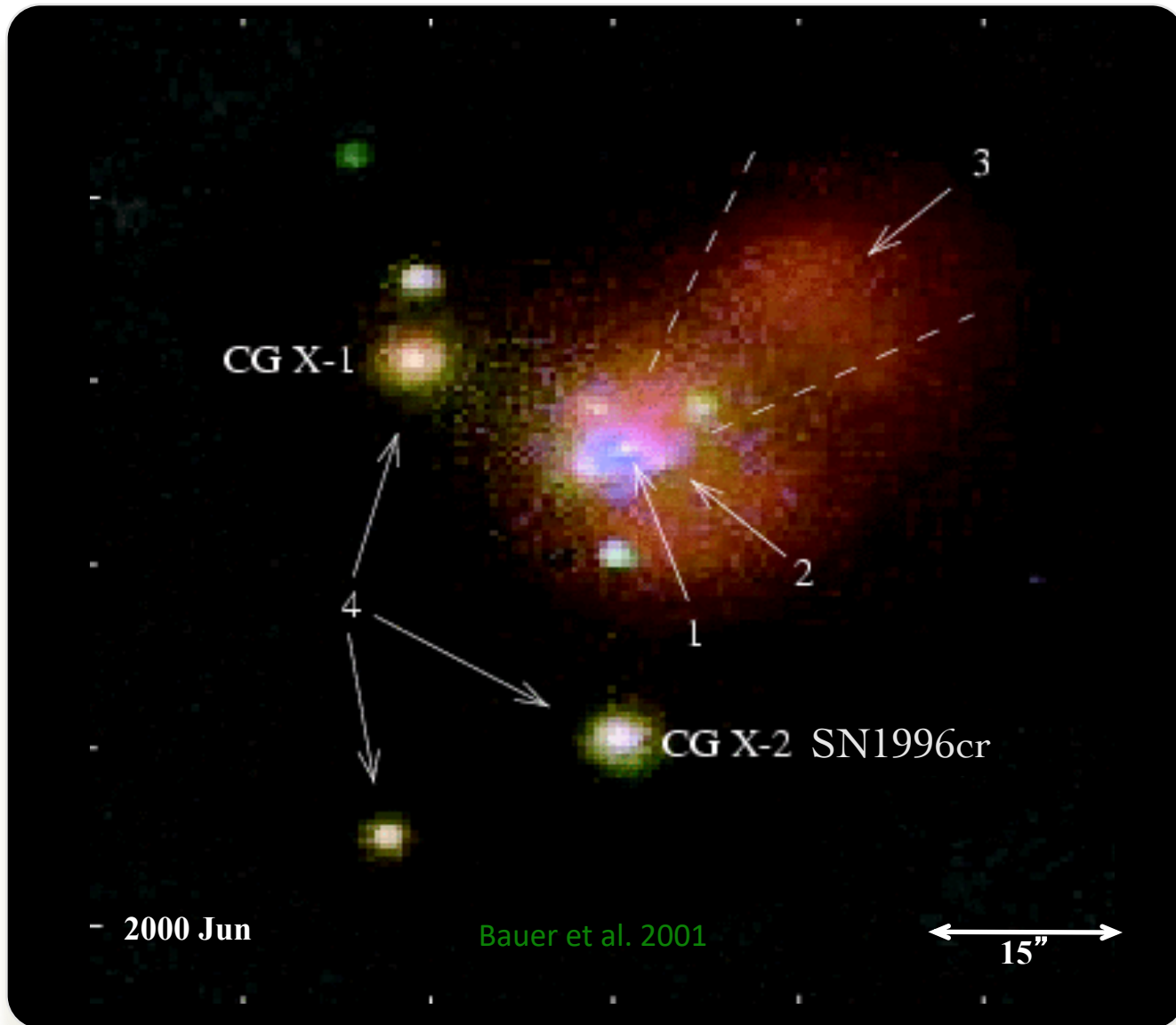
^d Richmond (1993).

X-Ray Emission from Supernovae (Schlegel 1995, Reports on Progress in Physics, 58, 1375)

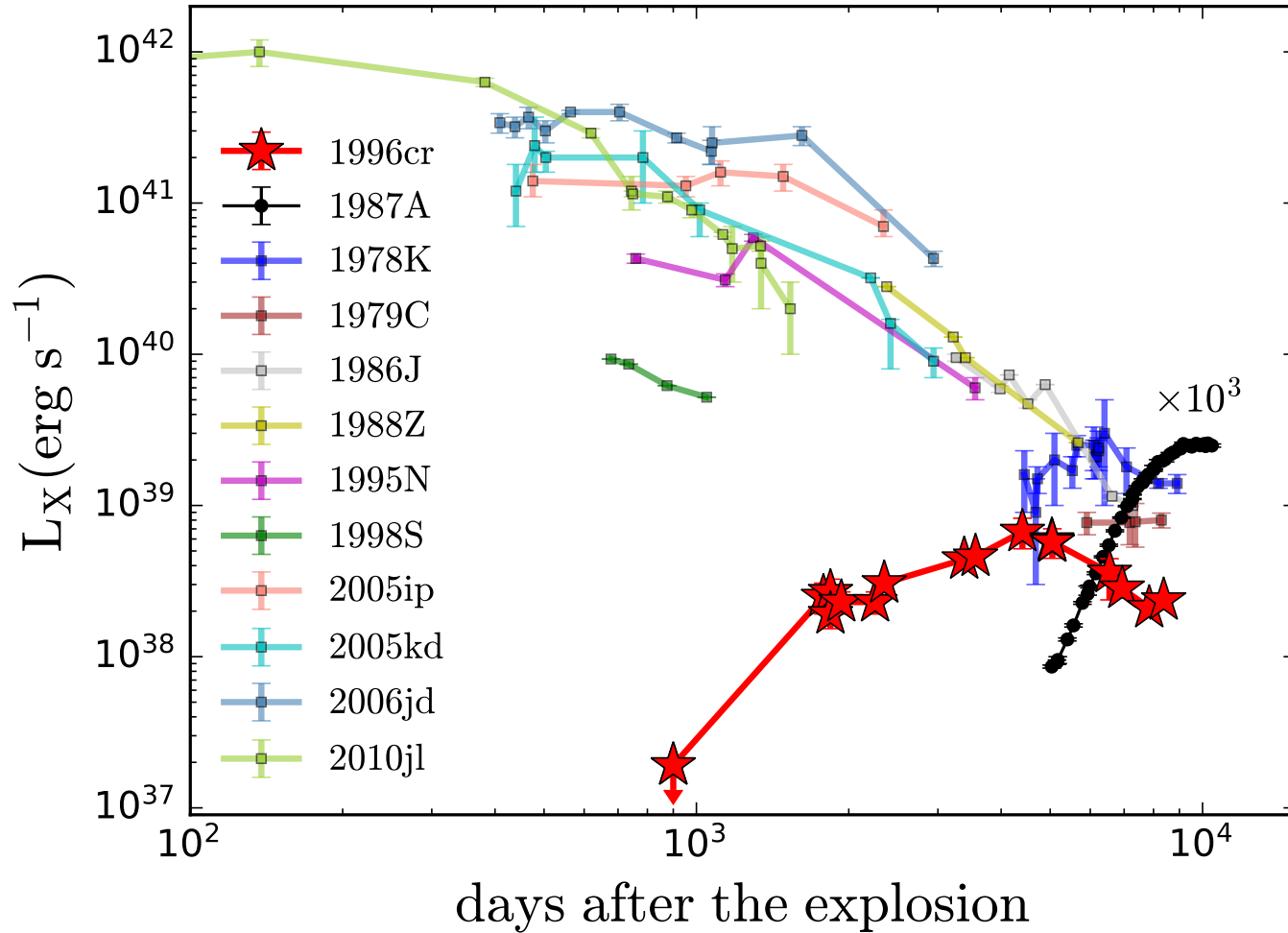


Rosat PSPSC
Spectrum of SN
1986J

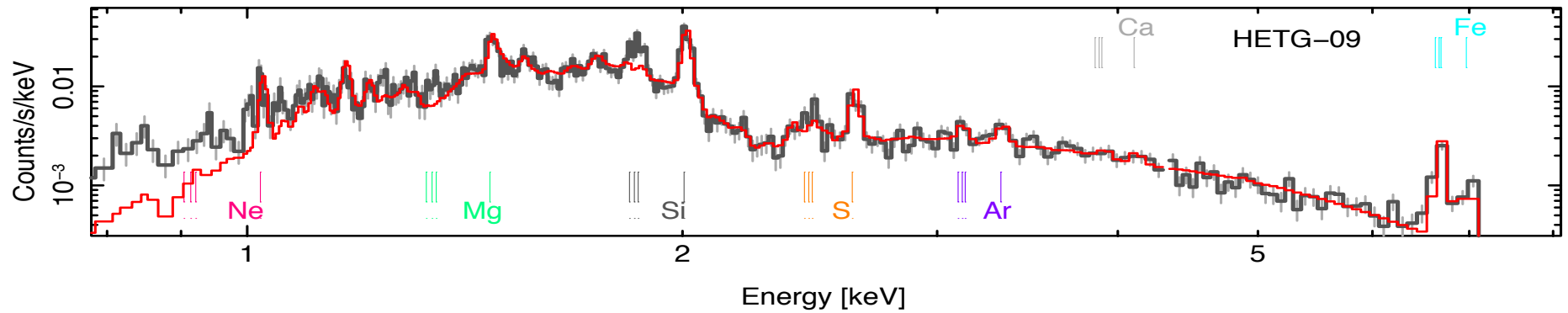
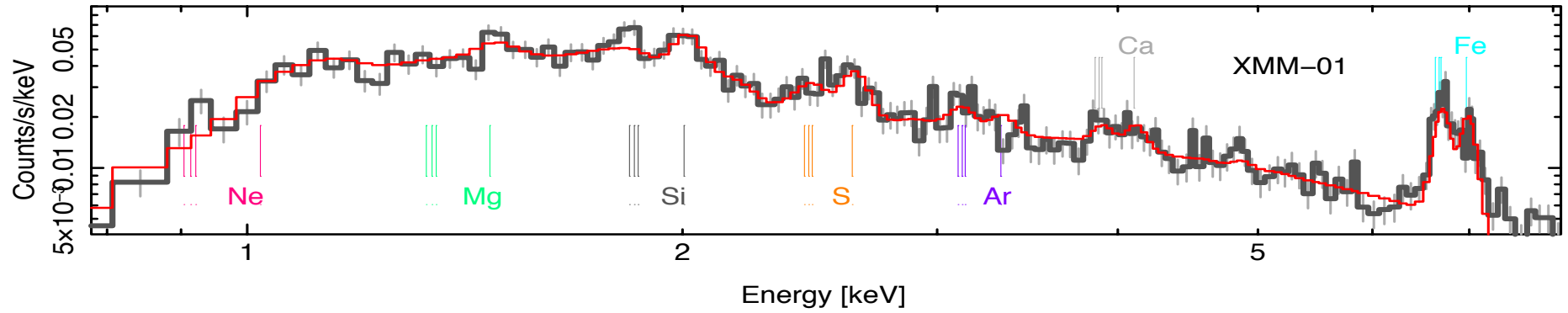
SN1996cr



SN 1996cr

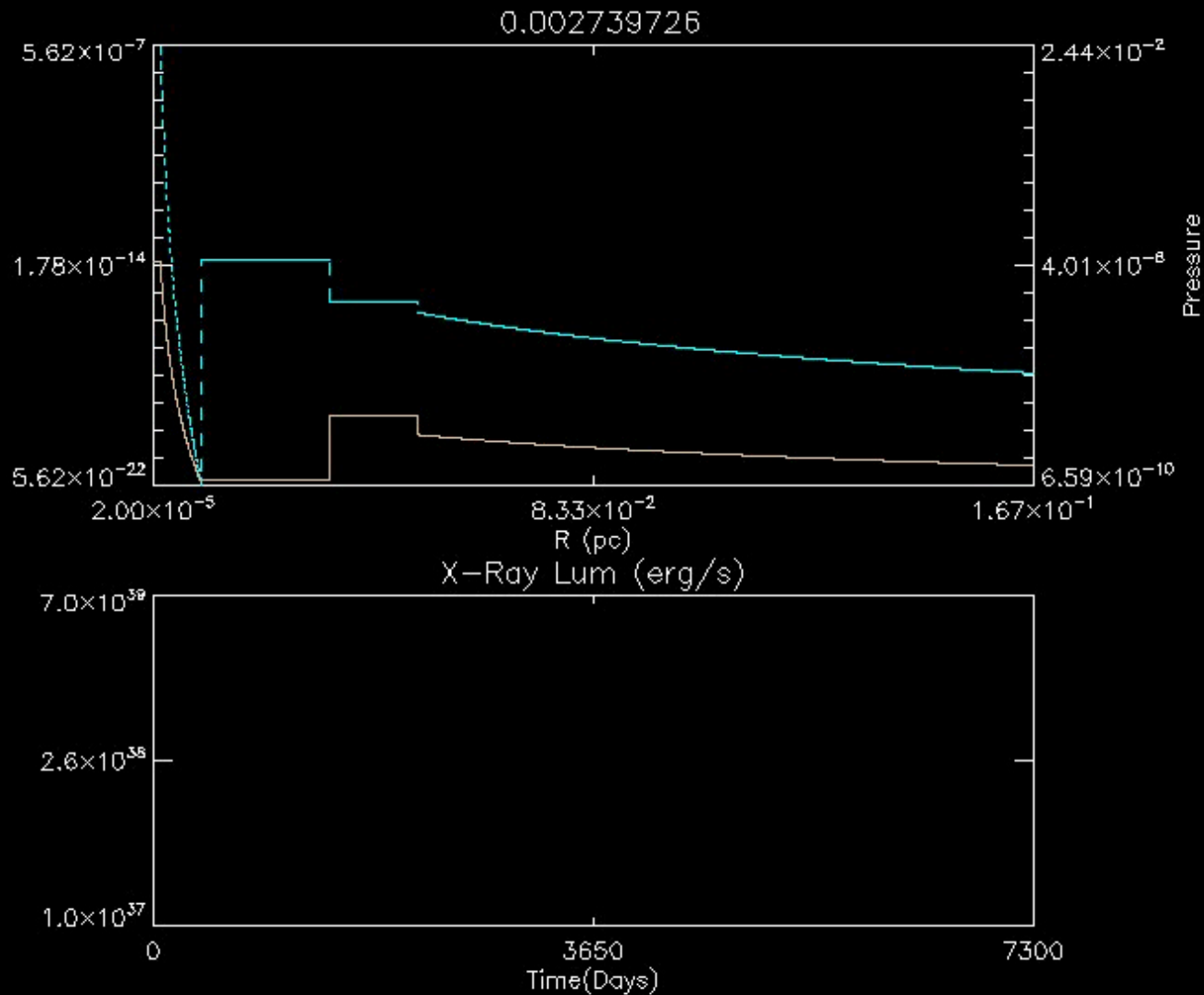


1996cr



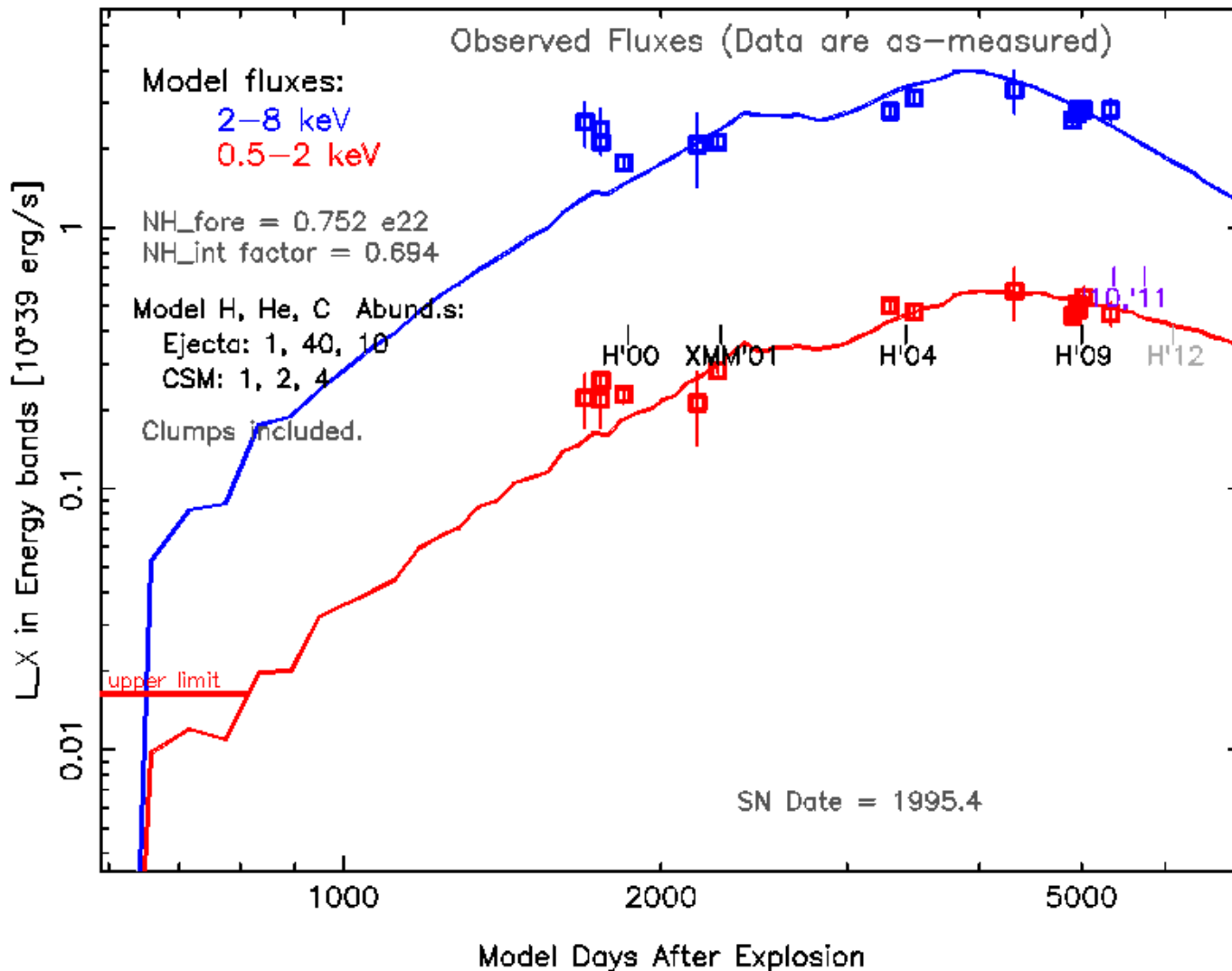
HETG 480 ks image

SN 1996cr (Hydro and X-ray)



1996cr - Comparison with X-Ray data

SN 1996cr: VH1 Model X-ray Light Curves (from files: 96cr_mar24/wrbub1nnn)

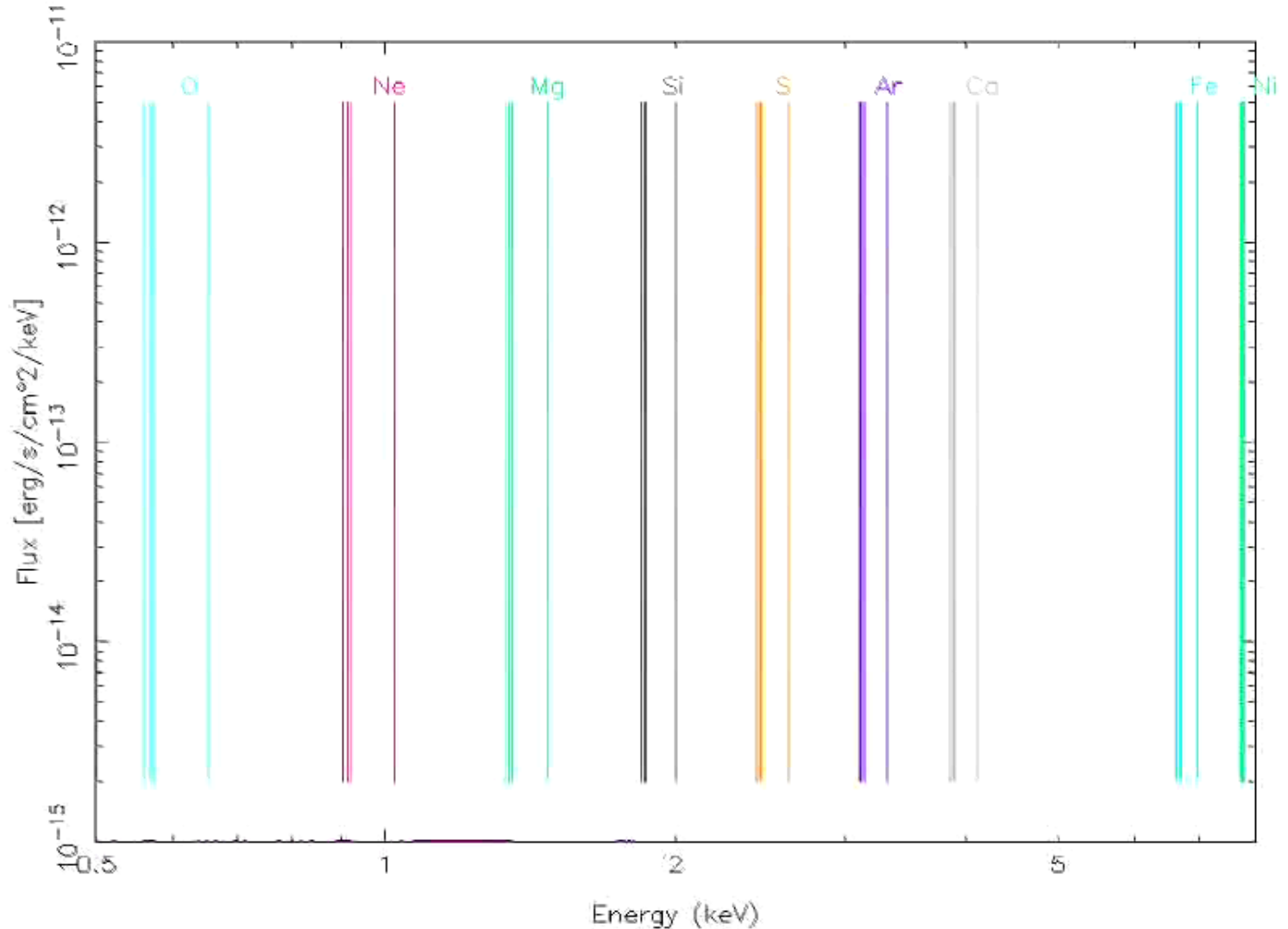


Dwarkadas, V. V.;
Dewey, D.; Bauer,
F, 2010, MNRAS,
407, 812

1996cr - Xray spectral evolution

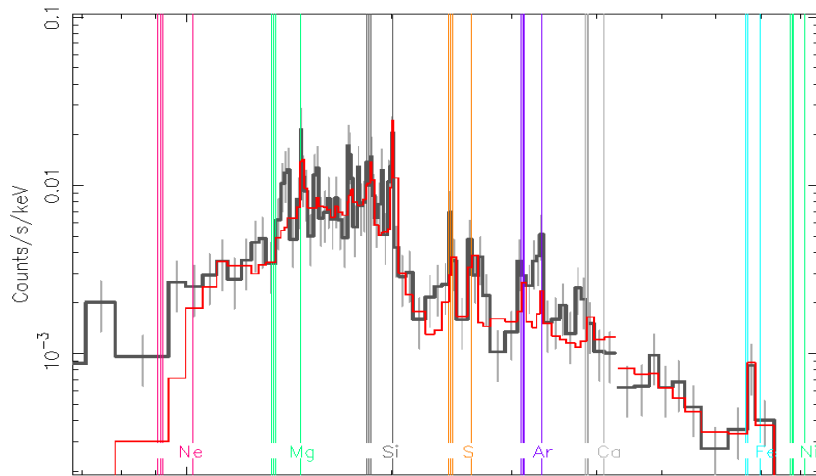
(Blue - CSM; Black - Ejecta; Red - Total)

Flux (0.5–8 keV) = 2.6505×10^{30} erg/s (96cr_mar24/wrbub.1001) Time = 0.32436 yr.s

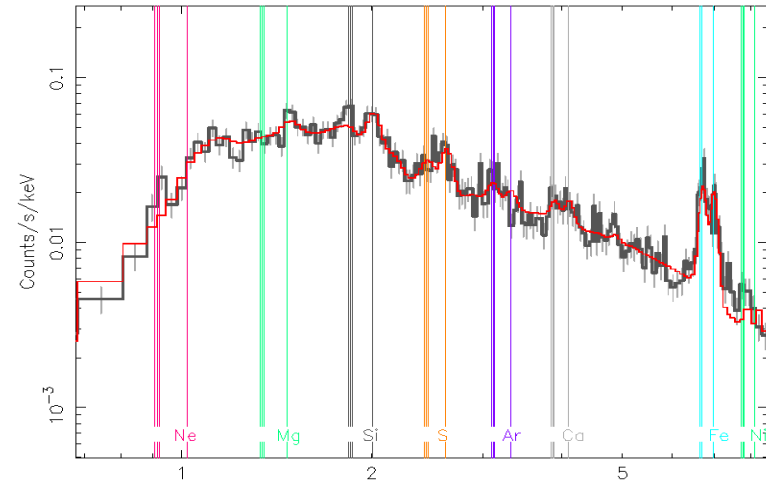


SN 1996cr (Comparison between Observed and Simulated Spectra)

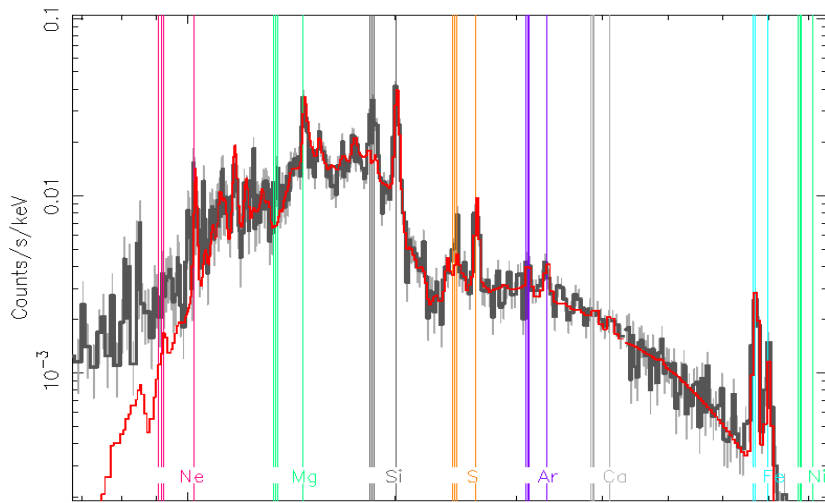
HETG-00 Data (Black) with Mar24-i34-Hydro Model (x1.36, Red)



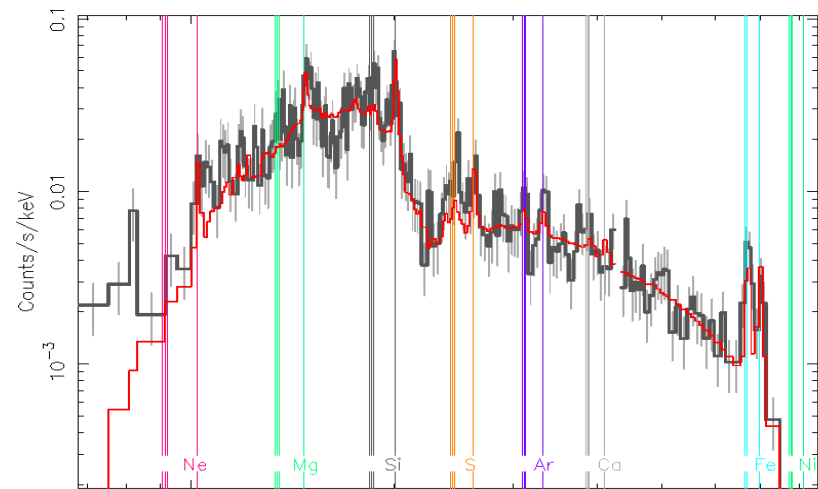
XMM-01nb Data (Black) with Mar24-i42-Hydro Model (x0.79, Red)



HETG-09 Data (Black) with Mar24-i79-Hydro Model (x1.13, Red)

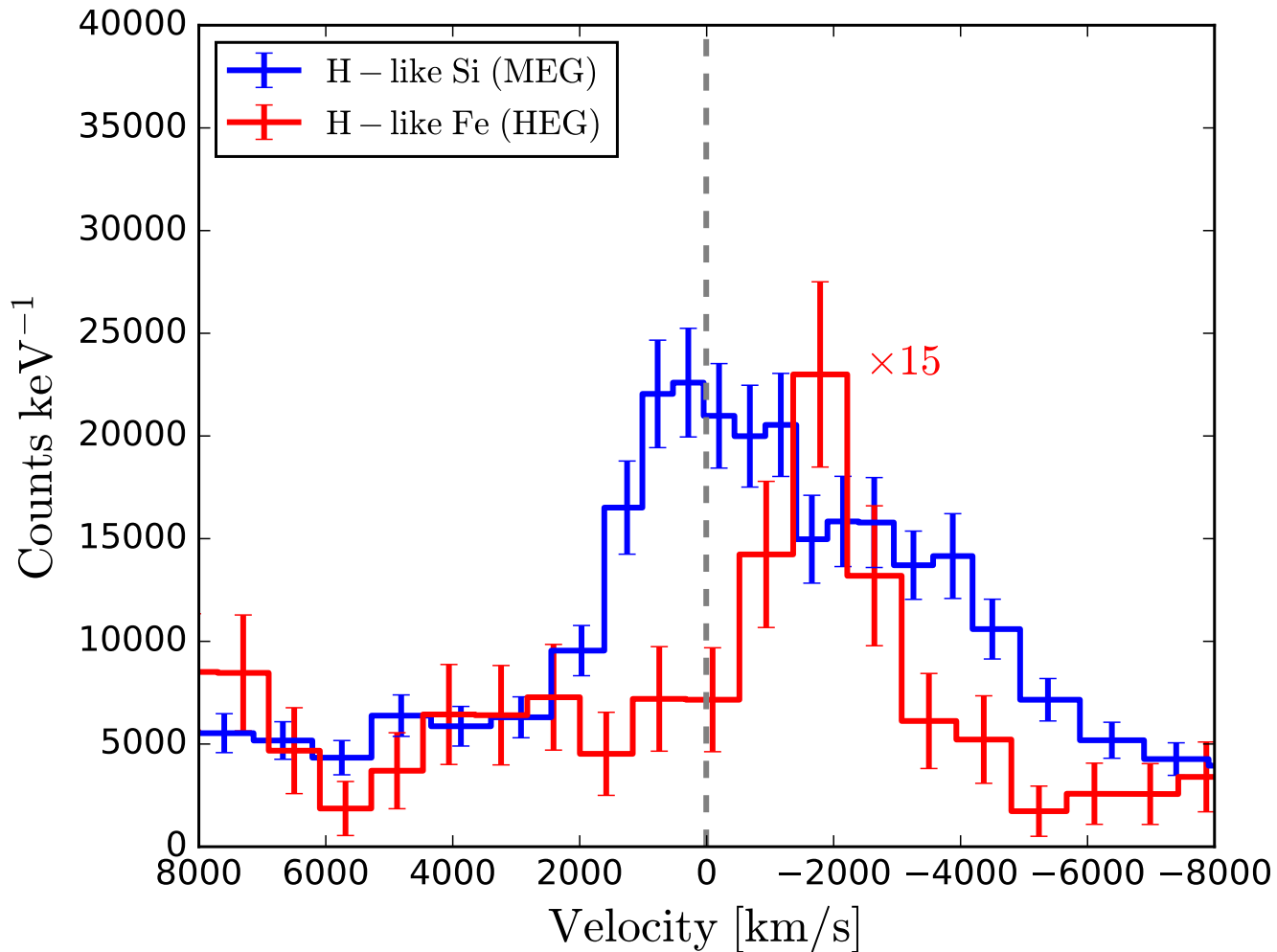


Energy [keV]



Energy [keV]

Si and Fe Line Profiles

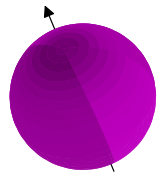


Asymmetric line profiles of H-like Si and H-like Fe profiles from 2009 HETG image.

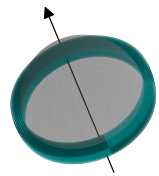
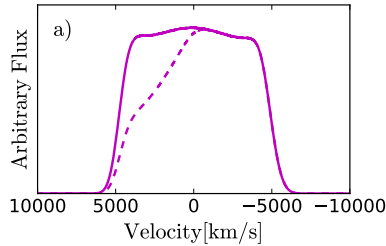
1. Profiles are clearly asymmetric
2. Distinct profiles imply different physical/geometrical origins

Shellblur Convolution Model

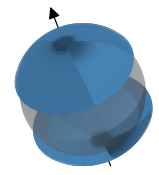
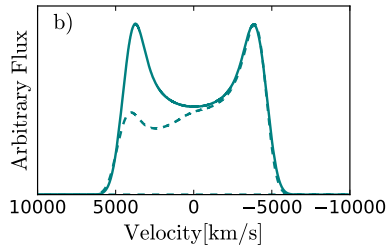
“shellblur” - spherical geometry parameterized by maximum velocity (v_{max}), inclination angle with respect to the line-of-sight (i), minimum and maximum aperture angles (θ_{min} , θ_{max}), and interior absorption term (N_{ejecta}).



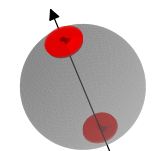
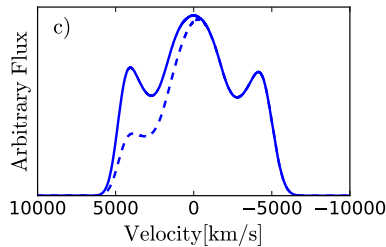
$\theta_{max} = 90^\circ$, $\theta_{min} = 0^\circ$



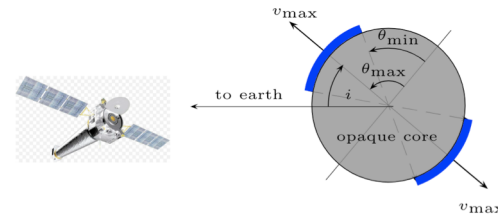
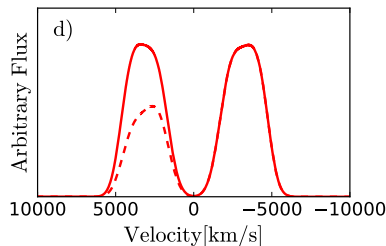
$\theta_{max} = 10^\circ$, $\theta_{min} = 0^\circ$



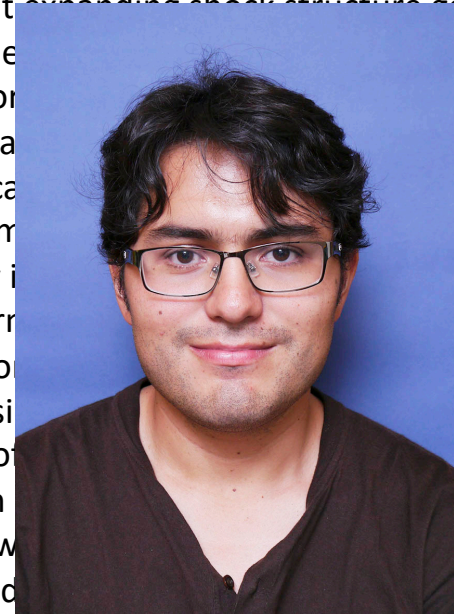
$\theta_{max} = 90^\circ$, $\theta_{min} = 30^\circ$



$\theta_{max} = 90^\circ$, $\theta_{min} = 70^\circ$



Examples of different expanding shell structure geometries, (a) spherically symmetric, (b) a 10-degree wide equatorial cap, (c) a 60-degree wide polar cap, (d) a 20-degree wide polar cap. In all cases, maximum velocity is 5000 km/s, axis of symmetry is along the line of sight, and a uniform density of ejecta is assumed. The maximum obscuration is 20% (shell diameter) to the far side of the shell. The input is an unresolved Gaussian line profile with a width of 20 km/s. Two line-profiles are shown for each geometry: one for an unobscured shell ($N_{ejecta} = 2 \times 10^{23} \text{ cm}^{-2}$, i.e., unobscured; solid curves) and one for an obscured shell ($N_{ejecta} = 2 \times 10^{23} \text{ cm}^{-2}$, i.e., obscured; dashed curves).

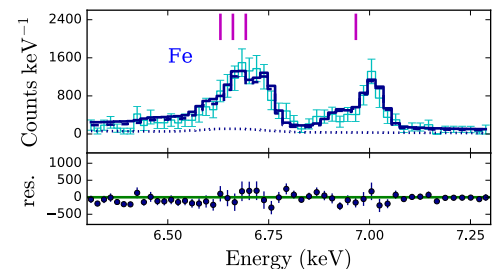
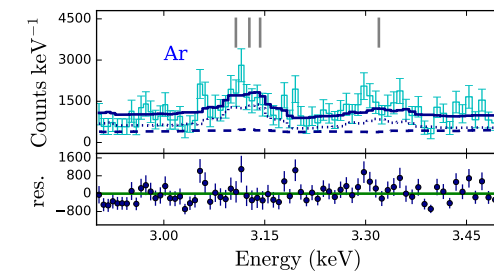
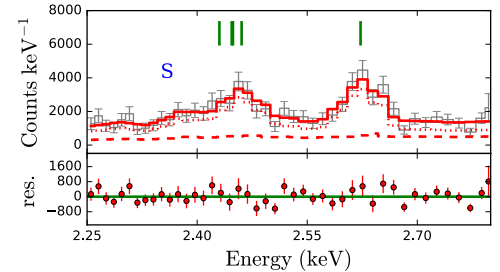
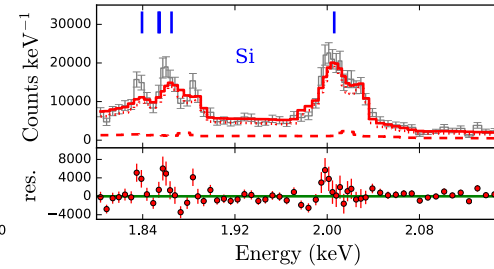
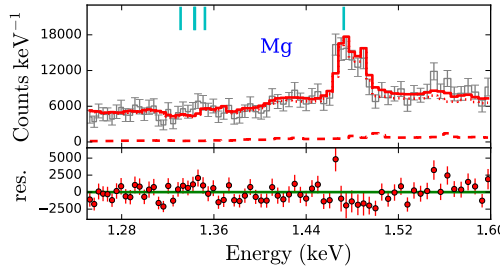
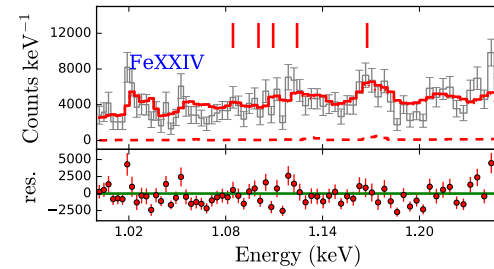
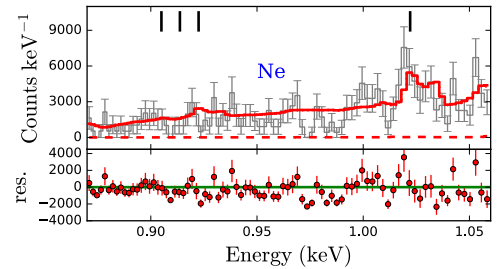
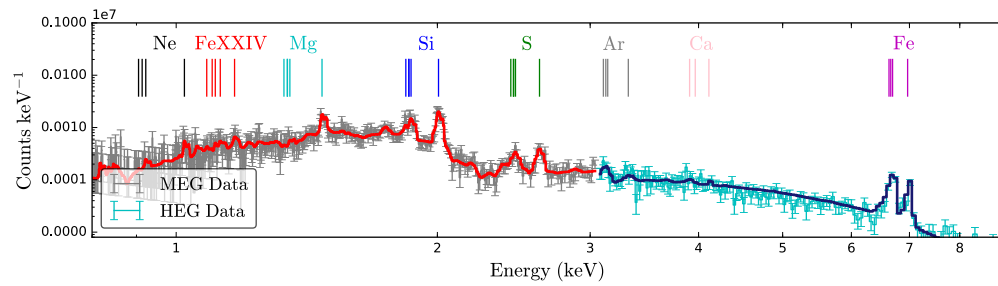


5000 km
the line
provides a
at the
shells show
an input
keV. Two
20

Best-Fit Model M5

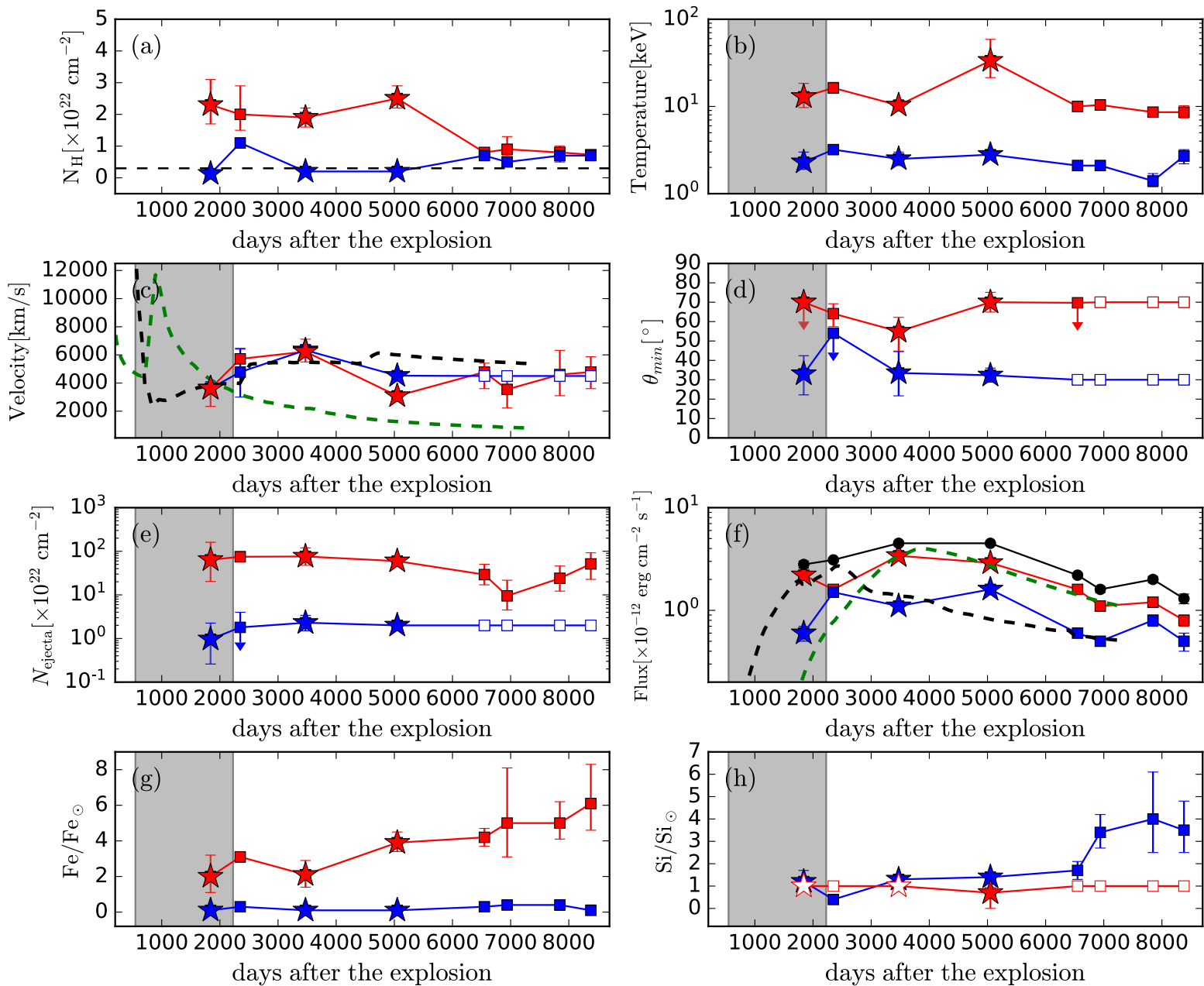
(two temperatures, two polar geometries, two absorptions) compared to the 2009 epoch spectra.

Close-up spectra of all detected H-like and He-like emission complexes and their residuals

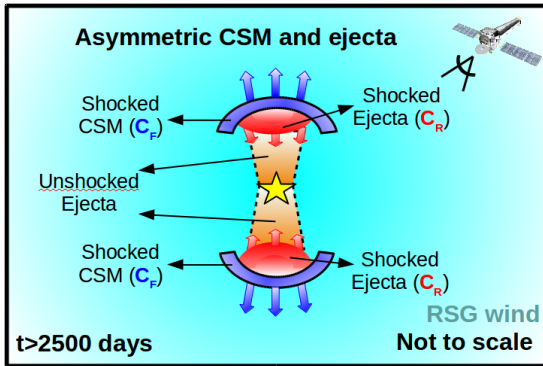
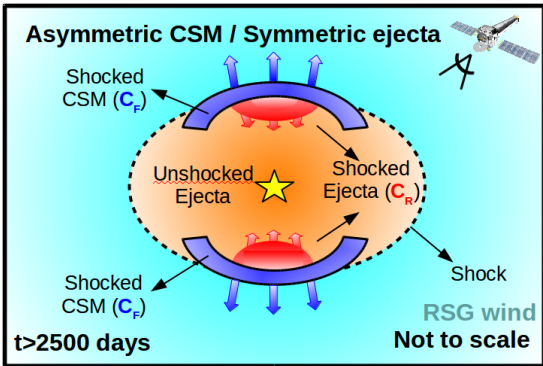
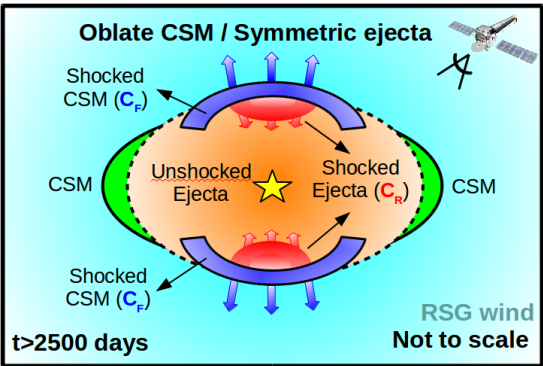
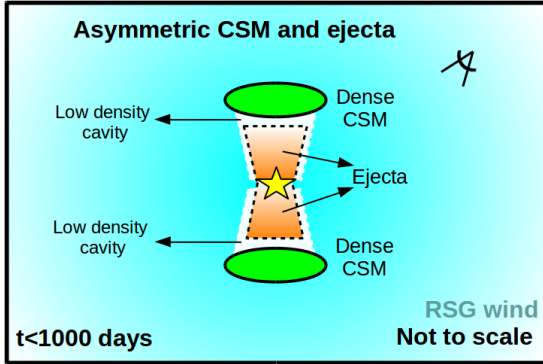
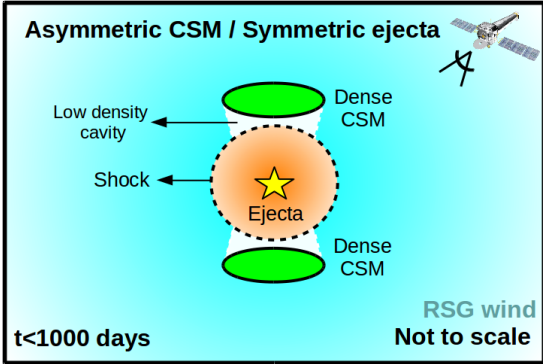
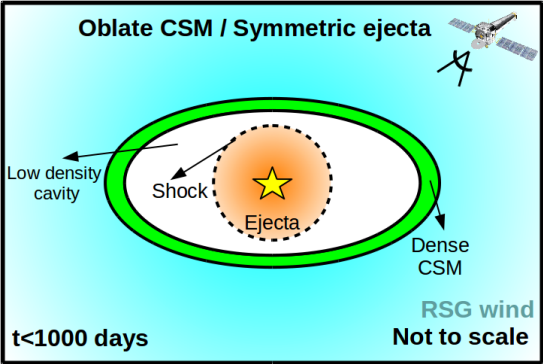


Quirola-Vásquez, J.; Bauer, F. E.; Dwarkadas, V. V. et al. 2019, MNRAS, 490, 4536

Evolution of parameters at different epochs. Red symbols and blue symbols denote parameters associated with the CR (high kT, high NH, narrow polar angle) and CF (low kT, low NH, wider polar angle) components, respectively.



Geometry



Conclusions

- SN 1996cr is a clear example of a SN expanding within a wind-blown bubble, similar to SN 1987A.
- Numerical hydrodynamic simulations, combined with synthetic spectral calculations, enable us to excavate the SN environment, trace the evolution of the shock wave within the circumstellar medium (CSM), and hone in on the SN progenitor.
- The superb HETG 480 ks spectrum allows resolution of velocity profiles of Ne, Mg, Si, S and Fe lines.
- For once we can accomplish in X-rays what SN optical astronomers do regularly - explore possible geometrical models to describe the line profile, provide new insights into the SN morphology, and monitor the line evolution as a tracer of the ejecta-CSM interaction.
- We find that the data are best fit by two components – a hotter component with high NH and a narrow polar angle, and a lower kT component with lower NH and wider polar angle.
- We tentatively identify these as consistent with the reverse shocked ejecta and forward shocked CSM.

Questions & Discussion